https://doi.org/10.15407/ujpe66.10.890

O.R. BARAN

Institute for Condensed Matter Physics, Nat. Acad. of Sci. of Ukraine
(1, Svientsitskogo Str., Lviv 79011, Ukraine; e-mail: ost@ph.icmp.lviv.ua)

ENERGY FLUX EFFECT IN THE ONE-DIMENSIONAL SPIN-$\frac{1}{2}$ XX MODEL OF MAGNETOELECTRIC. LAGRANGE MULTIPLIER METHOD

The Lagrange multiplier method is applied to study a nonequilibrium steady state with energy flux in the one-dimensional spin-$\frac{1}{2}$ XX model of a magnetoelectric with the Katsura–Nagaosa–Balatsky mechanism at sufficiently low temperatures. With the help of the Jordan–Wigner transformation, the problem is reduced to that with the Hamiltonian for spinless noninteracting fermions and can be solved exactly. A number of phase diagrams are plotted, and the dependences of the magnetization, electric polarization, and various susceptibilities on the magnetic and electric fields, as well as on the energy flux, are calculated.

K e y w o r d s: one-dimensional XX model, magnetoelectric, nonequilibrium steady states, energy flux, Lagrange multiplier method.

1. Introduction

1.1. Nonequilibrium steady states

In modern statistical physics, much attention is paid to the theoretical study of nonequilibrium stationary processes of various nature that take place in various systems and models. In particular, the specific features of nonequilibrium steady states (NESSs) were studied in the framework of the nonequilibrium spin-boson model [1, 2], the simplified model of a system of noninteracting electrons (a one-dimensional chain of fermions consisting of a central part and two metal thermostats) [2], the electron-hole-photon system [3], the finite quantum system of interacting particles connected to electrodes that are simultaneously thermostats [4], the quantum wire [5], the system in which a quantum dot is placed between a metal and a superconductor or a ferromagnetic contact with opposite polarizations [6], the XX chain located in a transverse field and connected to quantum reservoirs with noninteracting spins and different temperatures [7], and the spin models with interactions between the nearest neighbors and the energy [8–20] or spin [9, 21–24] current. It should be noted that the main specific feature of NESSs is the presence of a permanent flux of some physical quantity (energy, magnetic moment, charge, and so on).

For one-dimensional quantum systems, there are several methods to study NESSs. In particular, in works [16–18], the nonequilibrium system with the energy flux induced by the different temperatures, T_1 and T_2, of two parts of the chain was interpreted – making use of the effective Hamiltonian – as an equilibrium system (if the both temperatures do not equal zero) or as a system in the ground state (if any of those temperature equals zero). In works [5, 8–14], the Lagrange multiplier method was used. In this method, the state stimulated by the energy flux or the magnetic moment can be approximately generated as the ground state of the effective $\mathcal{H} - \lambda\mathcal{J}$ Hamiltonian (the Hamiltonian $\mathcal{H}$ of the system under consideration is supplemented with a term pro-

portional to the flux operator $\mathcal{J}$). This method is based on the fact that, when the flux is an integral of motion, i.e. $[\mathcal{H}, \mathcal{J}] = 0$. Then, the steady state can be described using the generalized Gibbs ensemble [14, 25, 26]. It should be noted that, for the systems in the nonequilibrium steady state in which the energy flux is induced by thermostats with different temperatures, the Lagrange multiplier method should be only implemented, when those temperatures are low, and their difference is small [10, 14].

Let us dwell briefly on the main results obtained while studying the properties of NESSs in the framework of one-dimensional spin models with energy flux. In works [8, 9], the main attention was focused on the study of pair correlation functions in the one-dimensional Ising model and the XX model, both in the transverse field. It was found that, in the states with energy flux, the correlations damp according to the power law as the distance between the sites grows. In work [9], it was also shown that the damping of the xx pair correlation function in the NESS occurs faster than in the state without energy flux. In work [10], it was established that, in the one-dimensional XX model, if the energy flux is switched on, the intensity redistribution of the xx dynamic structural factor takes place at low frequencies from the edge of the Brillouin zone toward its center. Let us recall that the conclusions made in works [8–10] are applicable only in the case of very low temperatures, because the studies were carried out on the basis of the Lagrange multiplier method. The authors of works [17, 18] used a method that has no restrictions on the temperatures of the chain parts. In work [17], it was shown that, in the XX model in the transverse field and at low temperatures, the xx correlation function damps with the distance according to the power law. At high temperatures, this correlation function damps exponentially at long distances and according to the power law at short ones. In work [18], the Casimir effect in the quantum spin chain with two magnetic impurities in the NESS was studied. It was found that the Casimir force damps exponentially with the growth of the distance between those impurities.

A special reference should also be made concerning works [27–30], where systems with energy flux were considered using the Lagrange multiplier method. However, they are not directly related to the study of nonequilibrium stationary processes. In particular, the properties of the ground state of the three-cubit one-dimensional XX model in the transverse field in the presence of an energy flux were studied in work [27]. In work [28], the quantum entanglement of two qubits interacting with the XY chain with energy flux was considered. The authors of work [29] studied how the energy flux affects the motion of the quantum state in the XX model in a homogeneous transverse field. The cited work, similarly to two previous ones, is related to quantum computers. The authors of work [30] considered a one-dimensional generalized model of a compass, in which the energy flux is an integral of motion only in particular cases. The influence of three-particle interactions and the Dzyaloshinsky–Moriya interaction on the physical characteristics was also studied.

1.2. Magnetoelectric effect

Compounds with the magnetoelectric effect (MEE), as well as the corresponding quantum spin or electronic models, continue to be the objects of extensive researches [31–40]. It should be noted here that, although the MEE was substantiated theoretically [41] and discovered experimentally [42] in the Cr_2O_3 compound as long as half a century ago, no microscopic explanation of this phenomenon has been done for a long time.

Currently, several mechanisms of the MEE formation in crystals have been proposed (see reviews [32, 34]). These are the magnetostriction model, the model of spin-dependent *p-d* hybridization of orbitals, and the model with the Katsura–Nagaosa–Balatsky (KNB) mechanism of the coupling between the localized spins (magnetic moments) and the electric bond polarization [43, 44]. In the latter model, the polarization emerges owing to the displacement of a ligand ion located between two magnetic ions, with the superexchange interaction taking place between those magnetic particles. Hence, the KNB mechanism is based on the assertion that the polarization at the bond between two magnetic ions is proportional to the spin current between them, which, in the operator representation, has the form of the Dzyaloshinsky–Moriya interaction for a number of spin systems. In this connection, the KNB models of magnetoelectrics are also often called the models of magnetic current or the inverse Dzyaloshinsky–Moriya interaction.

The Katsura–Nagaosa–Balatsky mechanism of the coupling between the localized magnetic moments

and the electric polarization of the bond between them was observed in a number of magnetic compounds, in particular, the one-dimensional magnetoelectric $CuCl_2$ [45]. In addition, $LiCu_2O_2$ [46] and $LiCuVO_4$ [47] crystals can also be described rather well in the framework of the one-dimensional KNB model.

Besides the fundamental importance of the MEE, it also opens wide opportunities for technological applications due to the mechanism allowing the control over the magnetic properties of materials (especially nanostructured) with the help of an electric field and vice versa [37, 39, 40, 48, 49], which is the main reason for a high interest in this effect. Here, we may mention the development of magnetoelectric-based data carriers that do not need electric currents [50], $BiFeO_3$-based optical diodes [51], and others. The latter example became possible because of the dynamic MEE, which is applied in a lot of domains [52–54]. In particular, under the laser action, there arises a spin current in magnetoelectrics because, according to the Floquet theory, strong periodic fields generate additional terms in the Hamiltonian, which allow the magnetoelectric bond to be dynamically controlled [52]. Such a spin current can be detected using opto-spintronic devices. Another interesting phenomenon is the dynamic phase transitions induced by ultrashort periodic pulsations of the electric field [54].

There are a few rigorous results for magnetoelectric systems, and, as far as we know, all they were obtained in the framework of one-dimensional models [55–60] or for two-dimensional decorated lattices [61]. A quantum spin-1/2 XXZ chain with the KNB mechanism of the coupling between magnetization and electric polarization was cosidered in work [55], where, in particular, the magnetization, electric polarization, and magnetoelectric tensor were analyzed as functions of the electric and magnetic fields. It was found that such a simple model does not predict the so-called nontrivial magnetoelectric effect, when only the electric (magnetic) field can induce the magnetization (electric polarization). This phenomenon can be described, only if additional interactions in the system are made allowance for. For instance, the above-mentioned nontrivial MEE is realized in the XX KNB chain with three-spin interactions [56].

Recently, the effect of a geometry change in the case of the XX magnetoelectric with the KNB mechanism in the zigzag chain [57] and the influence of the anisotropy on the magnetoelectric properties of the one-dimensional XY KNB model [58] have been studied. Additionally, exact results were obtained in work [59] for the KNB magnetoelectric on a ladder with the Ising and Heisenberg interactions in the chains and between them, respectively. A special mention should also be made of the one-dimensional model of a quantum compass, which was generalized to the case of the magnetoelectric with the KNB mechanism and solved exactly [60].

1.3. Formulation of the problem

In this research carried out in the framework of the Lagrange multiplier method, the influence of an energy flux on the parameters of the one-dimensional spin-$\frac{1}{2}$ XX model for the magnetoelectric in a nonequilibrium steady state in the electric and transverse magnetic fields is considered. The coupling of localized spins with the electric polarization of the bond is described in this model using the Katsura–Nagaosa–Balatsky mechanism. The energy flux can be induced, for example, by thermostats at the chain ends. The main attention is focused on the analysis of phase diagrams, as well as the dependences of the electrical polarization and susceptibilities (magnetic, electric, and magnetoelectric ones) on the fields and the energy flux.

Recall that the Lagrange multiplier method is pertinent to describe the NESS with a permanent energy flux in the case where the edges of the system are connected to thermostats with different and rather low temperatures. This method is based on the fact that such a nonequilibrium state with a permanent energy flux can be described by the generalized Gibbs distribution $\mathrm{e}^{-\overline{\beta}(\mathcal{H}-\lambda\mathcal{J}^{\mathcal{E}})}$, where $\overline{\beta}$ is the average value of the inverse temperatures of the tanks contacting with the chain edges, $\mathcal{H}$ is the chain Hamiltonian, $\mathcal{J}^{\mathcal{E}}$ is the energy flux operator, and λ is the field generating this flux [14].

It should be noted that the magnetoelectric model under consideration is integrable. In integrated models, the Fourier law is not obeyed, and the energy flux is not proportional to the temperature gradient in the spin chain [10, 62]. This circumstance may be associated with the fact that, in such systems, the energy flux is an integral of motion and, as a consequence, the thermal conductivity coefficients are anomalous [63, 64].

2. One-Dimensional Spin-$\frac{1}{2}$ XX Model of Magnetoelectric

A one-dimensional spin-$\frac{1}{2}$ XX model of a magnetoelectric in the electric field directed perpendicularly to the z-axis [$\mathbf{E} = (E^x, E^y, 0)$] and in a transverse magnetic field [$\mathbf{h} = (0, 0, h^z)$] is considered. The coupling of the electric polarization $\mathbf{p}_{j,j+1}$ of the bond connecting the spins $\mathbf{S}_j$ and $\mathbf{S}_{j+1}$ with those localized magnetic moments is described by the Katsura–Nagaosa–Balatsky mechanism [43]:

$$\mathbf{p}_{j,j+1} = \gamma \mathbf{e}_{j,j+1} \times \mathbf{S}_j \times \mathbf{S}_{j+1}. \tag{1}$$

Here, $\mathbf{e}_{j,j+1}$ is a unit vector oriented from the j-th site to the $(j+1)$-th one, and γ is the coupling coefficient between the electric polarization and the spin current operator. In what follows, for simplicity, we put $\gamma = 1$. Since the chain is oriented along the x-axis, i.e. $\mathbf{e}_{j,j+1} = (1, 0, 0)$, the chosen configuration of the fields ensures the problem integrability (the magnetoelectric with the energy flux taken into account on the basis of the Lagrange multiplier method).

The Hamiltonian of the one-dimensional XX magnetoelectric with the chosen fields $\mathbf{h}$ and $\mathbf{E}$ has the form [55–57, 65]

$$\mathcal{H}^{\rm ME} = \sum_{j=1}^{N} \Big[- hS_j^z + \mathcal{I}(S_j^x S_{j+1}^x + S_j^y S_{j+1}^y) - \\ - E(S_j^y S_{j+1}^x - S_j^x S_{j+1}^y) \Big], \tag{2}$$

where $h = h^z$ is the external transverse magnetic field, $\mathcal{I}$ is the superexchange interaction, $E = E^y$ is the y-component of the external electric field,

$$p_{j,j+1} = p_{j,j+1}^y \equiv S_j^y S_{j+1}^x - S_j^x S_{j+1}^y$$

is the operator of the y-component of the bond electrical polarization.

Recall that the quantity $S_j^y S_{j+1}^x - S_j^x S_{j+1}^y$ is the z-component of the Dzyaloshinsky–Moriya interaction [66, 67] in the operator form. Various models with it have been studied for decades [68–75] including the case where it is regularly variable [76, 77]. It should be noted that, for the one-dimensional spin-1/2 XY chain in a transverse field with the homogeneous Dzyaloshinsky–Moriya interaction directed along the z-axis, an exact result was obtained as long ago as in 1965 in work [68] on the basis of the one-dimensional Jordan–Wigner transformation.

3. Nonequilibrium Steady States

To study the nonequilibrium states of a magnetoelectric (2) with the stationary energy flux, the Lagrange multiplier, λ, method for quantum systems can be applied [8–14]. For instance, at the temperature $T \to 0$, such a steady state corresponds to the state with the lowest energy for model (2) with the given energy flux. In other words, we need to calculate the ground state of the following effective Hamiltonian:

$$\mathcal{H}^{\mathcal{E}} = \mathcal{H}^{\rm ME} - \lambda \mathcal{J}^{\mathcal{E}}, \tag{3}$$

where $\mathcal{J}^{\mathcal{E}}$ is the so-called macroscopic energy flux, and the Lagrange multiplier λ is an effective field that governs this flux.

The local energy flux $J_j^{\mathcal{E}}$, which contributes from the j-th spin into the "macroscopic" flux $\big(\mathcal{J}^{\mathcal{E}} = \\ = \sum_{j=1}^{N} J_j^{\mathcal{E}}\big)$, is obtained from the continuity equation for the local energy [8, 63, 64, 78–81],

$$\dot{H}_j^{\rm ME} = i[\mathcal{H}^{\rm ME}, H_j^{\rm ME}] = -{\rm div} J_j^{\mathcal{E}} = J_{j-1}^{\mathcal{E}} - J_j^{\mathcal{E}}. \tag{4}$$

Here, $H_j^{\rm ME}$ is the operator of this local energy, and we put $\hbar = 1$.

For our problem, the operator $H_j^{\rm ME}$ can be selected in the form

$$H_j^{\rm ME} = \mathcal{I}(S_j^x S_{j+1}^x + S_j^y S_{j+1}^y) - hS_j^z - \\ - E(S_j^y S_{j+1}^x - S_j^x S_{j+1}^y). \tag{5}$$

Note, firstly, that this is not the only way to select the local energy operator that provides the fulfillment of the continuity equation (4). Secondly, the correct choice of $H_j^{\rm ME}$ (i.e., it provides the fulfillment of Eq. (4)) does not affect the final result for the "macroscopic" energy flux.

On the basis of Eqs. (4) and (5), we obtain the following local energy flux operator:

$$J_j^{\mathcal{E}} = hE(S_j^x S_{j+1}^x + S_j^y S_{j+1}^y) + \\ + h\mathcal{I}(S_j^y S_{j+1}^x - S_j^x S_{j+1}^y) + \\ + 2E\mathcal{I}(S_j^x S_{j+1}^z S_{j+2}^x + S_j^y S_{j+1}^z S_{j+2}^y) + \\ + (E^2 - \mathcal{I}^2)(S_j^x S_{j+1}^z S_{j+2}^y - S_j^y S_{j+1}^z S_{j+2}^x). \tag{6}$$

Hence, Hamiltonian (3) can be written in the form

$$\mathcal{H}^{\mathcal{E}} = \sum_{j=1}^{N} \Big[- hS_j^z + \tilde{\mathcal{I}}(S_j^x S_{j+1}^x + S_j^y S_{j+1}^y) - \\ - \tilde{E}(S_j^y S_{j+1}^x - S_j^x S_{j+1}^y) +$$

$$+\tilde{K}(S^x_{j-1}S^z_jS^x_{j+1}+S^y_{j-1}S^z_jS^y_{j+1})+$$
$$+\tilde{R}(S^x_{j-1}S^z_jS^y_{j+1}-S^y_{j-1}S^z_jS^x_{j+1})\Big], \quad (7)$$

where the following notations were introduced:

$$\tilde{\mathcal{I}}=\mathcal{I}-\lambda hE, \quad \tilde{E}=E+\lambda h\mathcal{I},$$
$$\tilde{K}=-2\lambda E\mathcal{I}, \quad \tilde{R}=-\lambda(E^2-\mathcal{I}^2).$$

It should be noted that the spin chains in which, in addition to two-spin interactions between the nearest neighbor sites, there are three-spin interactions between the next after the nearest sites have been studied theoretically for several decades. One of the first works, where the so-called modified XXZ model with competing interactions whose Hamiltonian is the sum of two integrals of motion was considered, is [82]. One of the integrals of motion is the well-known XXZ chain, and another one is the chain with only three-spin interactions. It should be noted that the latter integral of motion is nothing else but the energy flux operator for the ordinary one-dimensional XXZ model (see, e.g., work [83]). Similar zigzag ladders with competing interactions between the nearest and the next after the nearest neighbors were studied in works [83–87] and many others.

4. Result of the Jordan–Wigner Fermionization

The effective Hamiltonian (7) with energy flux has the same two- and three-spin terms as in work [56]. Therefore, we can immediately write down the final result obtained after the one-dimensional Jordan–Wigner transformation (see works [65, 88–90]) and, after changing to the momentum space,

$$\mathcal{H}^{\mathcal{E}}=\sum_{-\pi\le k<\pi}\Lambda_k\left(n_k-\frac{1}{2}\right). \quad (8)$$

Here, k belongs to the first Brillouin zone, $n_k=c^\dagger_kc_k$, $c^\dagger_k$ and c_k are the creation and annihilation operators, respectively, of spinless fermions, and the spectrum is determined as follows:

$$\Lambda_k=-h+\tilde{\mathcal{I}}\cos k-\tilde{E}\sin k-\frac{\tilde{K}}{2}\cos(2k)+$$
$$+\frac{\tilde{R}}{2}\sin(2k). \quad (9)$$

In the thermodynamic limit and on the basis of Eq. (8), it is easy to calculate the energy of the ground state per one site,

$$e_0=\frac{\langle\mathcal{H}^{\mathcal{E}}\rangle}{N}=-\frac{1}{4\pi}\int\limits_{-\pi}^{\pi}dk|\Lambda_k|, \quad (10)$$

and, on the basis of Eq. (10), the energy flux at $T\to0$,

$$\langle J^{\mathcal{E}}\rangle=\frac{\langle\mathcal{J}^{\mathcal{E}}\rangle}{N}=-\frac{\partial e_0}{\partial\lambda}=-\frac{1}{4\pi}\int\limits_{-\pi}^{\pi}dk\,\mathrm{sgn}(\Lambda_k)g_k, \quad (11)$$

where the notation

$$g_k=hE\cos k+h\mathcal{I}\sin k-$$
$$-E\mathcal{I}\cos(2k)+\frac{E^2-\mathcal{I}^2}{2}\sin(2k) \quad (12)$$

was introduced.

The magnetization and electrical polarization (per one site) at the zero temperature can be obtained, e.g., as follows:

$$m\equiv\lim_{N\to\infty}\frac{1}{N}\sum_{j=1}^{N}\langle S^z_j\rangle=\frac{1}{2\pi}\int\limits_{-\pi}^{\pi}dk\left(\langle n_k\rangle-\frac{1}{2}\right)=$$
$$=-\frac{1}{4\pi}\int\limits_{-\pi}^{\pi}dk\,\mathrm{sgn}(\Lambda_k), \quad (13)$$

$$p\equiv\lim_{N\to\infty}\frac{1}{N}\sum_{j=1}^{N}\langle p_{j,j+1}\rangle=\frac{1}{2\pi}\int\limits_{-\pi}^{\pi}dk\,\langle n_k\rangle\sin k=$$
$$=-\frac{1}{4\pi}\int\limits_{-\pi}^{\pi}dk\,\mathrm{sgn}(\Lambda_k)\sin k. \quad (14)$$

In our study, the independent parameters of the problem are the energy flux (rather than λ; see, e.g., work [9] and Appendix), the superexchange interaction, and the magnetic and electric fields. In this case, the spectrum of elementary excitations (9) is given parametrically: $\Lambda_k=\Lambda(k,\lambda,\mathcal{I},h,E)$, where $\lambda=\lambda(\langle J^{\mathcal{E}}\rangle,\mathcal{I},h,E)$ is an implicitly determined function (see Eq. (11)). Accordingly, other physical characteristics will also be determined parametrically.

A numerical analysis of spectrum (9) shows that, depending on the values of the parameters $\langle J^{\mathcal{E}}\rangle$, $\mathcal{I}$, h, and E, there can be two or four Fermi points k^{F}_ν. Recall (see, e.g., works [85,90,91]) that the points k^{F}_ν are

the quasimomentum values at which the spectrum of elementary excitations Λ_k equals zero. Note that if λ, $\mathcal{I}$, h, and E are independent parameters, there can also be two or four Fermi points. However, the case is also possible, where there is a gap in the spectrum [65].

On the basis of relations (9) and (11)–(14), and taking the presence of Fermi points

$$k_\nu^{\rm F}(\langle J^{\mathcal{E}}\rangle,\mathcal{I},h,E)=k_\nu^{\rm F}(\lambda(\langle J^{\mathcal{E}}\rangle,\mathcal{I},h,E),\mathcal{I},h,E),$$

into account, we obtain the magnetic, $\frac{\partial m}{\partial h}$, electric $\frac{\partial p}{\partial E}$, and two magnetoelectric, $\frac{\partial m}{\partial E}$ and $\frac{\partial p}{\partial h}$, susceptibilities at $T\to 0$:

$$\frac{\partial m}{\partial \xi}=\zeta\sum_\nu(-1)^\nu\frac{\partial k_\nu^{\rm F}}{\partial\xi}, \tag{15}$$

$$\frac{\partial p}{\partial \xi}=\zeta\sum_\nu(-1)^\nu\sin k_\nu^{\rm F}\frac{\partial k_\nu^{\rm F}}{\partial\xi}. \tag{16}$$

Here, the summation is carried out over the indices of all Fermi points, the notation $\zeta=\mathrm{sgn}(\Lambda_{k=\pi})/(2\pi)$ was introduced, and $\xi=h$ or E (here and below). We also present expressions (15) and (16), which are necessary for the calculation of susceptibilities, in the explicit form,

$$\frac{\partial k_\nu^{\rm F}}{\partial\xi}=-\left(\frac{\partial\Lambda_{k_\nu^{\rm F}}}{\partial\xi}+\frac{\partial\Lambda_{k_\nu^{\rm F}}}{\partial\lambda}\frac{\partial\lambda}{\partial\xi}\right)\Big/\left(\frac{\partial\Lambda_k}{\partial k}\Big|_{k=k_\nu^{\rm F}}\right), \tag{17}$$

$$\begin{aligned}\frac{\partial\lambda}{\partial\xi}=&-\left[\frac{1}{4\pi}\int\limits_{-\pi}^{\pi}dk\,\mathrm{sgn}(\Lambda_k)\frac{\partial g_k}{\partial\xi}+\right.\\&\left.+\zeta\sum_\nu(-1)^\nu g_{k_\nu^{\rm F}}\left(\frac{\partial\Lambda_{k_\nu^{\rm F}}}{\partial\xi}\right)\Big/\left(\frac{\partial\Lambda_k}{\partial k}\Big|_{k=k_\nu^{\rm F}}\right)\right]\times\\&\times\left[\zeta\sum_\nu(-1)^\nu g_{k_\nu^{\rm F}}\left(\frac{\partial\Lambda_{k_\nu^{\rm F}}}{\partial\lambda}\right)\Big/\left(\frac{\partial\Lambda_k}{\partial k}\Big|_{k=k_\nu^{\rm F}}\right)\right]^{-1},\end{aligned} \tag{18}$$

$$\frac{\partial\Lambda_k}{\partial h}=-1-\lambda(E\cos k+\mathcal{I}\sin k),$$

$$\frac{\partial\Lambda_k}{\partial E}=\lambda[\mathcal{I}\cos(2k)-E\sin(2k)-h\cos k]-\sin k,$$

$$\begin{aligned}\frac{\partial\Lambda_k}{\partial\lambda}=&-h(E\cos k+\mathcal{I}\sin k)+\mathcal{I}E\cos(2k)-\\&-(E^2-\mathcal{I}^2)\sin(2k)/2,\end{aligned}$$

$$\frac{\partial\Lambda_k}{\partial q}=-\tilde{\mathcal{I}}\sin k-\tilde{E}\cos k+\tilde{K}\sin(2k)+\tilde{R}\cos(2k),$$

$$\frac{\partial g_k}{\partial h}=E\cos k+\mathcal{I}\sin k,$$

$$\frac{\partial g_k}{\partial E}=h\cos k-\mathcal{I}\cos(2k)+E\sin(2k).$$

5. Results of Numerical Researches

In this section, the attention will be focused on the study of the dependences of the magnetization, electric polarization, and susceptibilities on the magnetic and electric fields, as well as on the energy flux. Since

- the fields h and E can be scaled by the interaction magnitude $|\mathcal{I}|$, the energy flux $\langle J^{\mathcal{E}}\rangle=\frac{1}{N}\langle\mathcal{J}^{\mathcal{E}}\rangle$ by the $\mathcal{I}^{\,2}$-value, and the Lagrange multiplier λ by the value of $1/|\mathcal{I}\,|$;
- $\langle J^{\mathcal{E}}\rangle$ is an even function of both the fields and interaction; the magnetization is an even function of E and $\mathcal{I}$, and an odd function of h; and the polarization has the following properties at a fixed energy flux:

$$p(\mathcal{I},h,E)=p(-\mathcal{I},-h,E)=-p(\mathcal{I},-h,-E),$$

then, without losing the generality, we may put $\mathcal{I}=-1$ and confine the consideration to positive magnetic fields $h\geq 0$ for an arbitrary E, or vice versa, for positive electric fields $E\geq 0$ for an arbitrary h.

Note that we carry out a theoretical study of the influence of the energy flux on the characteristics of the spin-$\frac{1}{2}$ XX model of the magnetoelectric with the KNB mechanism in the framework of the Lagrange multiplier method. Therefore, for the completeness of the picture, the values of $\langle J^{\mathcal{E}}\rangle$ will be analyzed in a rather wide interval.

5.1. Phase diagrams

Similarly to what was done in work [9], we will distinguish three different phases in the gapless spin fluid: nonmagnetic ($m=0$) phase I with four Fermi points, and magnetically ordered ($m\neq 0$) phases II and III with four and two Fermi points, respectively. The phase transitions between those phases can only be of the second kind. The difference between magnetically ordered phases II and III will be clarified in more details, when analyzing the field dependences of the magnetization, electric polarization, and susceptibilities.

Figures 1 to 3 exhibit the phase diagrams in the planes $(|h|,\langle J^{\mathcal{E}}\rangle)$, $(|E|,\langle J^{\mathcal{E}}\rangle)$, and $(|E|,|h|)$, respectively. Figure 1 demonstrates how the $(|h|,\langle J^{\mathcal{E}}\rangle)$ diagrams change with the variation of the electric field. They are qualitatively identical at any E-value and have a topology similar to that given and analyzed in work [9] for the XX model in the transverse magnetic field. All three phases are present in those phase diagrams. The boundary between phases II and III is

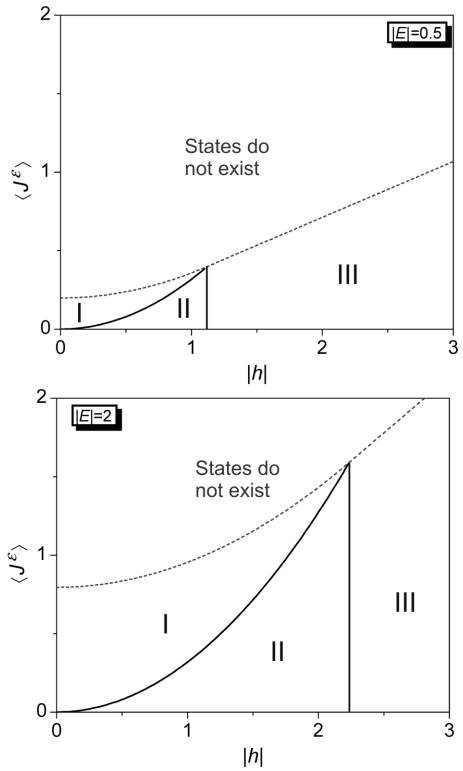

Fig. 1. Phase diagrams in the plane "magnetic field magnitude–energy flux" at various electric field magnitudes: $|E| = 0.5$ and 2. Also shown are the curves that correspond to the maximum achievable energy flux $\langle J^{\mathcal{E}}_{\max}\rangle$, with no states above them. The diagram for $E = 0$ can be seen in work [9], where it was shown that the transition between the magnetically ordered phases II and III occurs at $\left|h_c^{\mathrm{II}\to\mathrm{III}}\right| = 1$

a vertical segment. Besides the curves corresponding to the I → II and II → III phase transitions and converging at a point of the "triple point" (TP) kind, the phase diagrams contain curves corresponding to the maximum achievable energy flux $\langle J^{\mathcal{E}}_{\max}(|h|,|E|)\rangle$ (see work [9]). There are no states above those curves, because states with energy fluxes larger than $\langle J^{\mathcal{E}}_{\max}\rangle$ cannot be realized at the given magnetic and electric fields (see work [65] and Appendix). It should be noted that the "triple point" is not a classical triple point in this problem, because it lies on a curve that outlines the area, where the states do not exist.

It is also worth noting that the curves corresponding to the I → II phase transition in the $(|h|,\langle J^{\mathcal{E}}\rangle)$ diagrams are superimposed on one another at different electric field values. Furthermore, the smaller $|E|$, the "shorter" this curve. Thus, the coordinates

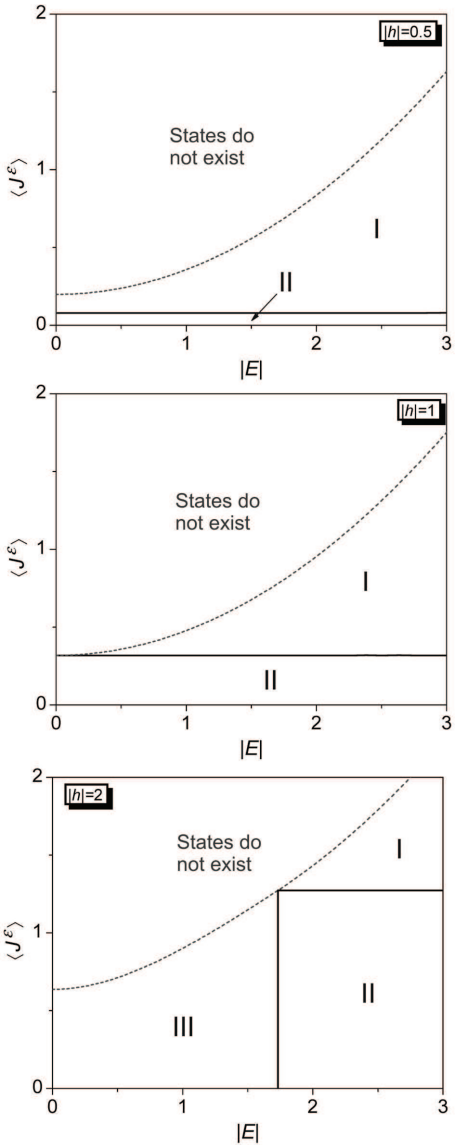

Fig. 2. Phase diagrams in the plane "electric field magnitude–energy flux" at various magnetic field magnitudes: $|h| = 0.5$, 1, and 2. Also shown are the curves that correspond to the maximum achievable energy flux $\langle J^{\mathcal{E}}_{\max}\rangle$, with no states above them

$(h_c^{\mathrm{I}\to\mathrm{II}}, \langle J^{\mathcal{E}}\rangle_c^{\mathrm{I}\to\mathrm{II}})$ of the transition points between phases I and II do not depend on the electric field value.

For the phase diagrams in the $(|E|,\langle J^{\mathcal{E}}\rangle)$ plane, there are three different topologies (see Fig. 2). In particular, in the diagrams for $|h| < 1$, the curve (boundary) between phases I and II does not intersect the curve corresponding to the maximum achievable

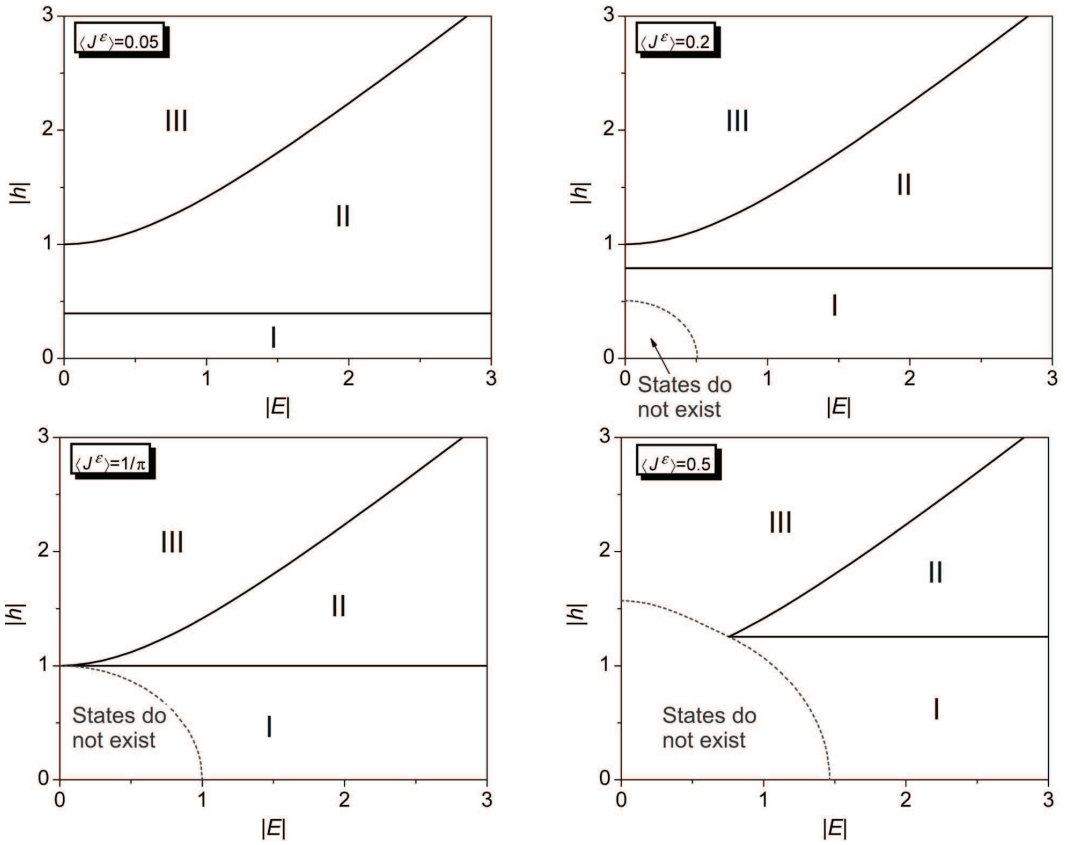

Fig. 3. Phase diagrams in the plane "electric field magnitude–magnetic field magnitude" at various energy flux values: $\langle J^{\mathcal{E}}\rangle = 0.05,\ 0.2,\ 1/\pi$, and 0.5. Also shown are the curves at every point of which the maximum achievable energy flux $\langle J^{\mathcal{E}}_{\max}\rangle$ is equal to the corresponding given flux value $\langle J^{\mathcal{E}}\rangle = 0.2,\ 1/\pi,\ 0.5$. There are no states below those curves

flux, whereas, at $|h| = 1$, those curves converge at the point $E = 0$, $\langle J^{\mathcal{E}}\rangle = 1/\pi$. In contrast to the cases with $|h| \le 1$, in the phase diagrams for $|h| > 1$, there are phase III and the "triple point". This TP shifts toward larger $|E|$ and $\langle J^{\mathcal{E}}\rangle$ as $|h|$ grows. It should be noted that the lines corresponding to the phase transitions between phases II and I (III) are horizontal (vertical).

The phase diagrams in the $(|E|, |h|)$ plane can possess four different topologies (see Fig. 3). If $\langle J^{\mathcal{E}}\rangle < 1/\pi$, the curves separating phases I, II, and III do not intersect, and only if $\langle J^{\mathcal{E}}\rangle < 1/(2\pi)$, there are no areas without states in the diagrams. Already in the case $\langle J^{\mathcal{E}}\rangle = 1/\pi$, there exists a "triple point" with the coordinates $(E_{\rm TP} = 0, |h_{\rm TP}| = 1)$. As the energy flux increases, this "triple point" shifts toward larger $|E|$ and $|h|$ (see the curves for $\langle J^{\mathcal{E}}\rangle = 1/\pi$ and 0.5 in Fig. 3). It should be noted that the coordinates $(E_c^{\rm II\to III}, h_c^{\rm II\to III})$ of the transition point between phases II and III do not depend on $\langle J^{\mathcal{E}}\rangle$, except for the case $\langle J^{\mathcal{E}}\rangle > 1/\pi$ where the transition curve between the mentioned phases begins from the "triple point". In other words, the curve corresponding to the II $\to$ III phase transitions at $\langle J^{\mathcal{E}}\rangle = 0.5$ is superimposed on the corresponding curves at $\langle J^{\mathcal{E}}\rangle = 0.05,\ 0.2$, and $1/\pi$ (it can be seen in Fig. 3).

5.2. Magnetization and electric polarization

Now, let us consider the behavior of the magnetization m and the electric polarization p, when the model parameters h, E, and $\langle J^{\mathcal{E}}\rangle$ change. Figures 4 to 6 depict almost all possible (qualitatively different) dependences of m and p on the magnetic and electric fields, as well as on the energy flux. It should be marked at once that, in our study, we did not consider cases where at least one of the $|h|$, $|E|$, or

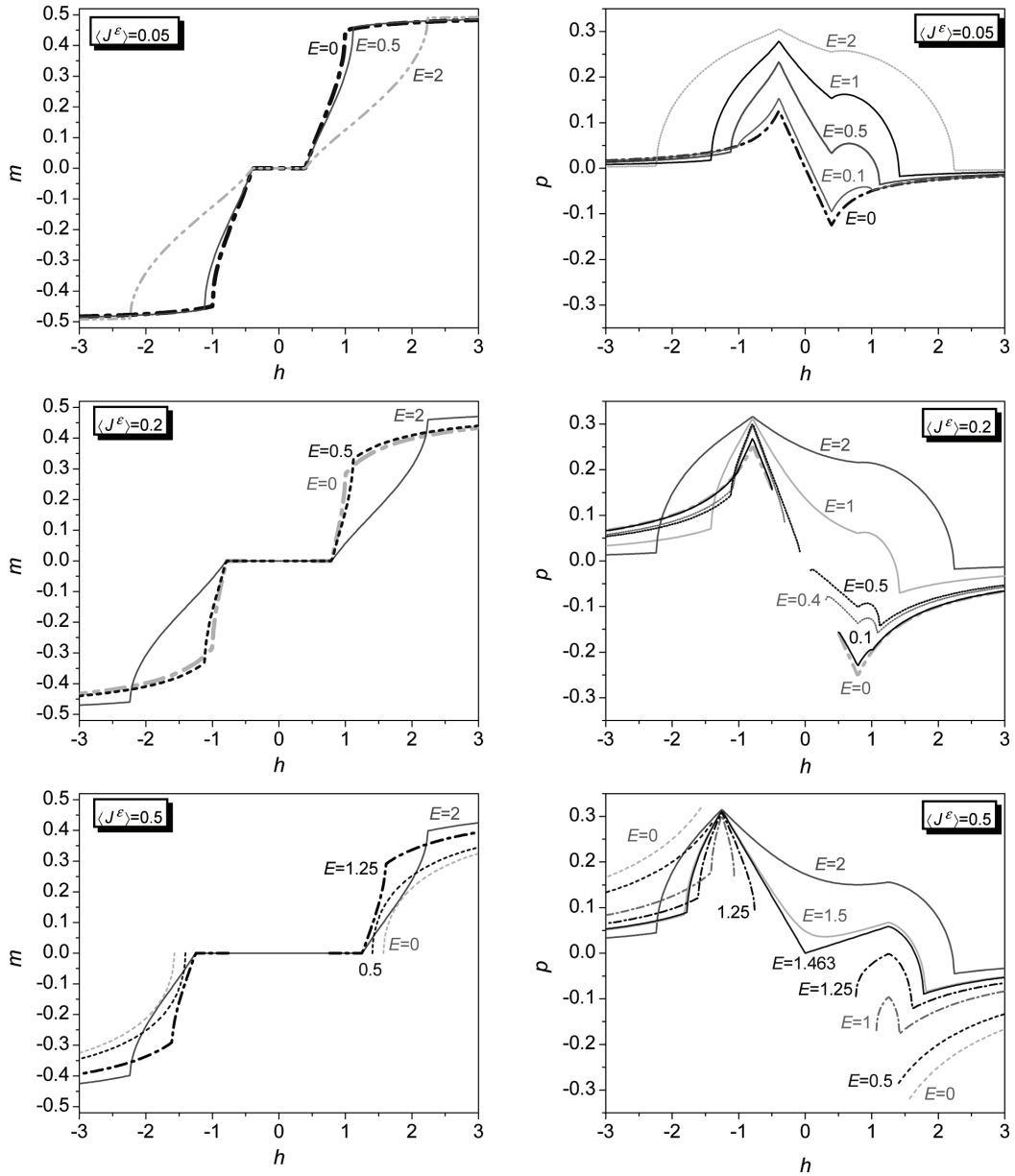

Fig. 4. Dependences of the magnetization m and the electric polarization p on the magnetic field for various values of the energy flux and the electric field. The upper, middle, and lower figures correspond to $\langle J^{\mathcal{E}} \rangle = 0.05$, 0.2, and 0.5, respectively

$\langle J^{\mathcal{E}} \rangle$ parameters is infinitely large. It is clear from the figures that, at the phase transition points, both the magnetization and the electric polarization dependences have cusps. Only the cusps corresponding to the transition between phases II and III in the dependences $p(h)$ in the case of electric fields close to zero are weakly pronounced (see Fig. 4).

It should be noted that the effective Hamiltonian (7) contains terms describing three-spin interactions $XZY - YZX$ and $XZX + YZY$, which lead to the spontaneous magnetization in the models considered in works [56, 85, 92] even in the absence of the magnetic field, as well as to the spontaneous electric polarization in the model studied in work [56] even in

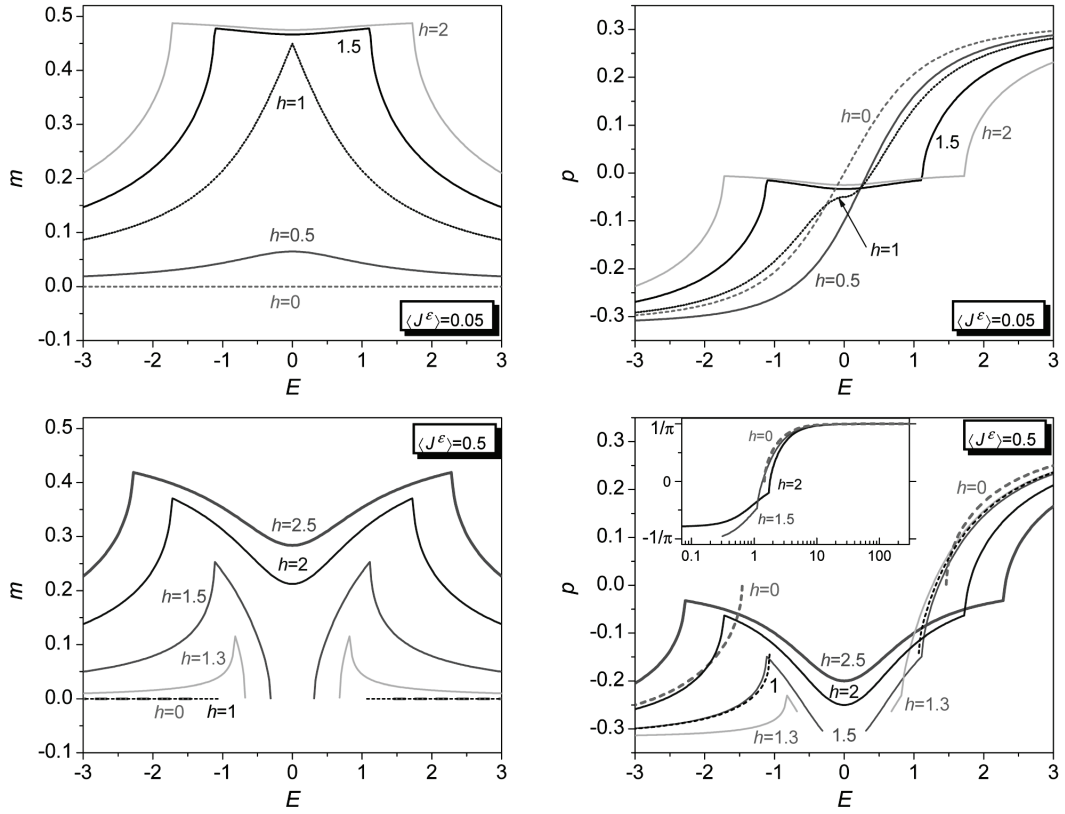

Fig. 5. Dependences of the magnetization m and the electric polarization p on the electric field for various values of the energy flux and the magnetic field. The upper and lower figures correspond to $\langle J^{\mathcal{E}} \rangle = 0.05$ and 0.5, respectively

the zero electric field. Due to those effects, as well as because the quantities h and E in our problem are included in a certain way into $\tilde{K}$, $\tilde{R}$, $\tilde{\mathcal{I}}$, and $\tilde{E}$, the dependences $p(h)$ and $p(E)$ are asymmetric. At the same time, the dependences $m(h)$ and $m(E)$ are symmetric (see Figs. 4 and 5).

At sufficiently low values of the energy flux (e.g., $\langle J^{\mathcal{E}} \rangle = 0.05$, see Figs. 1, 3, and 4), the system demonstrates a cascade of four phase transitions III $\to$ II $\to$ $\to$ I $\to$ II $\to$ III with the change of h at any E, and the behavior of the dependence $p(h)$ in phase II is drastically different in the cases of positive and negative h. In particular, for positive magnetic field values, the electric polarization in phase II can be a nonmonotonic function of h with one maximum, or a monotonically increasing function of h in the case where the electric field is close to zero. At the same time, if $h < 0$, the dependence $p(h)$ can only be a monotonically increasing function in the phase-II region at any value of the electric field. It should also be noted that if $\langle J^{\mathcal{E}} \rangle = 0.05$, the electric polarization in the magnetically disordered phase I can only be a decreasing function of h.

If $\langle J^{\mathcal{E}} \rangle = 0.2$ (see Figs. 1, 3, and 4), then, in contrast to the case $\langle J^{\mathcal{E}} \rangle = 0.05$, the given value of the energy flux ($\langle J^{\mathcal{E}} \rangle = 0.2$) cannot be achieved at the low h and E fields (as was said above), i.e. there is a region with no states. Therefore, when h grows, the system undergoes a cascade of four phase transitions III $\to$ II $\to$ I $\to$ II $\to$ III, only if $E > 0.5066$, whereas, at lower electric field values, we have two cascades of two transitions, III $\to$ II $\to$ I and I $\to$ II $\to$ III. In phase II, the $p(h)$ dependences at various E are similar to the corresponding dependences at $\langle J^{\mathcal{E}} \rangle = 0.05$: the electrical polarization in phase II at the positive h can be an increasing or nonmonotonic function of the magnetic field, whereas, at $h < 0$, it can only be monotonically increasing. In phase I, the behavior of $p(h)$ in the case $\langle J^{\mathcal{E}} \rangle = 0.2$ differs from the corresponding behavior at $\langle J^{\mathcal{E}} \rangle = 0.05$. In particular, the

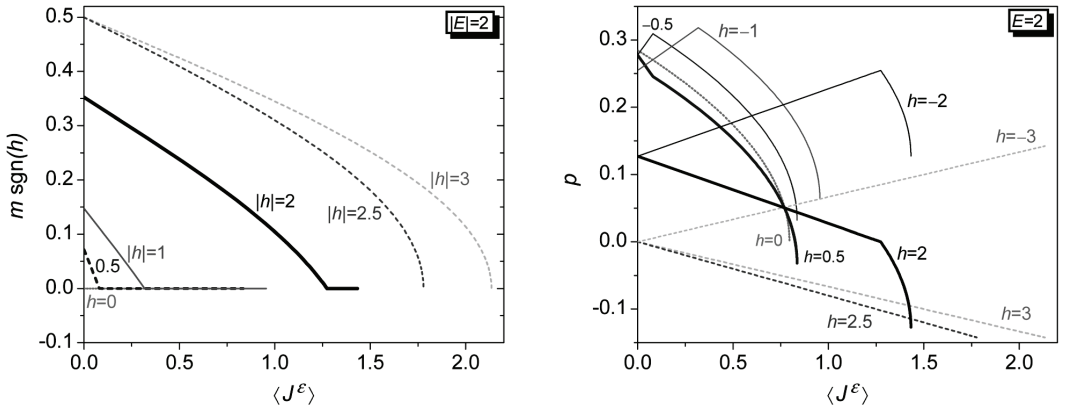

Fig. 6. Dependences of the magnetization m and the electric polarization p on the energy flux for various magnetic field values. The figures for m and p correspond to the cases $|E| = 2$ and $E = 2$, respectively

electric polarization is a decreasing function of h in this magnetically disordered phase only at large and very small values of the electric field. At the same time, e.g., at $E = 0.1$, 0.4, and 0.5, it is a decreasing function of the magnetic field in the nonmagnetic phase only if $h < 0$, whereas $p(h)$ is a nonmonotonic function with one maximum, if $h > 0$.

In the case of large energy flux values – e.g., $\langle J^{\mathcal{E}} \rangle = 0.5$ (see Figs. 1, 3, and 4) – there is a cascade of four phase transitions III $\to$ II $\to$ I $\to$ II $\to$ $\to$ III in the system, as h increases at $E > 1.4634$, and two cascades of phase transitions III $\to$ II $\to$ I and I $\to$ II $\to$ III at $E_{\rm TP} < E < 1.4634$ ($E_{\rm TP} = 0.7555$), whereas, at $E < E_{\rm TP}$, the system can be only in phase III. The electric polarization in phase II for negative h is a monotonically increasing function of the magnetic field for an arbitrary E (similarly to the cases $\langle J^{\mathcal{E}} \rangle = 0.05$ and 0.2 described above). At the same time, in contrast to the cases $\langle J^{\mathcal{E}} \rangle = 0.05$ and 0.2, the polarization $p(h)$ in phase II at $h > 0$ can only be a monotonically decreasing function, if the energy flux values are large. In the magnetically disordered phase I, the polarization behavior at $\langle J^{\mathcal{E}} \rangle = 0.5$ also differs from the corresponding behavior both at $\langle J^{\mathcal{E}} \rangle = 0.05$ and 0.2. In particular, for $E = 2$, 1.5, and 1.463, the polarization $p(h)$ is a nonmonotonic function with one minimum, and, for $E = 1.25$ and 1, it is monotonically decreasing (increasing) in regions I, if $h < 0$ ($h > 0$).

All the aforesaid about the polarization dependences on the magnetic field in the nonmagnetic (I) and magnetically ordered (II) phases concerns only the cases of finite $E \geq 0$. The behavior of $p(h)$ at finite negative E can be seen from the property $p(\mathcal{I}, h, E) = -p(\mathcal{I}, -h, -E)$, which takes place, if the energy flux is fixed.

At the same time, in the magnetically ordered phase III, in contrast to phases I and II, the polarization dependence on the magnetic field is unambiguous at any finite values of the energy flux and the electric field E (irrespective of its sign): $p(h)$ is a monotonically increasing function for both positive and negative h. It should be noted that, only in this magnetic phase III, the electric polarization is an even function of the electric field, ($p(\langle J^{\mathcal{E}} \rangle, \mathcal{I}, h, E) = p(\langle J^{\mathcal{E}} \rangle, \mathcal{I}, h, -E)$). This can be seen in Fig. 4, if we recall the property $p(\langle J^{\mathcal{E}} \rangle, \mathcal{I}, h, E) = -p(\langle J^{\mathcal{E}} \rangle, \mathcal{I}, -h, -E)$. But this behavior will be demonstrated more clearly below, when analyzing the dependences of p on E (Fig. 5).

Note that, for the given electric field and the energy flux at the region boundary with no states, we have $p(h) = -p(-h)$. This can be seen in Fig. 4 for $\langle J^{\mathcal{E}} \rangle = 0.2$ at $E = 0$, 0.1, 0.4, and 0.5, and for $\langle J^{\mathcal{E}} \rangle = 0.5$ at $E = 0$, 0.5, 1, and 1.25. In the case where the system is in phase III ($\langle J^{\mathcal{E}} \rangle = 0.5$, $E = 0$ and 0.5), this relationship can be explained, in particular, on the basis of the property $p(\langle J^{\mathcal{E}} \rangle, \mathcal{I}, h, E) = -p(\langle J^{\mathcal{E}} \rangle, \mathcal{I}, -h, -E)$ and the fact that the polarization is an even function of the electric field in this phase III.

The dependences of the magnetization on the magnetic field are rather trivial for any $\langle J^{\mathcal{E}} \rangle$. In the magnetically ordered phases II and III, the dependence $m(h)$ is an increasing function. It is worth noting the magnetization dependence in the case of large $\langle J^{\mathcal{E}} \rangle$

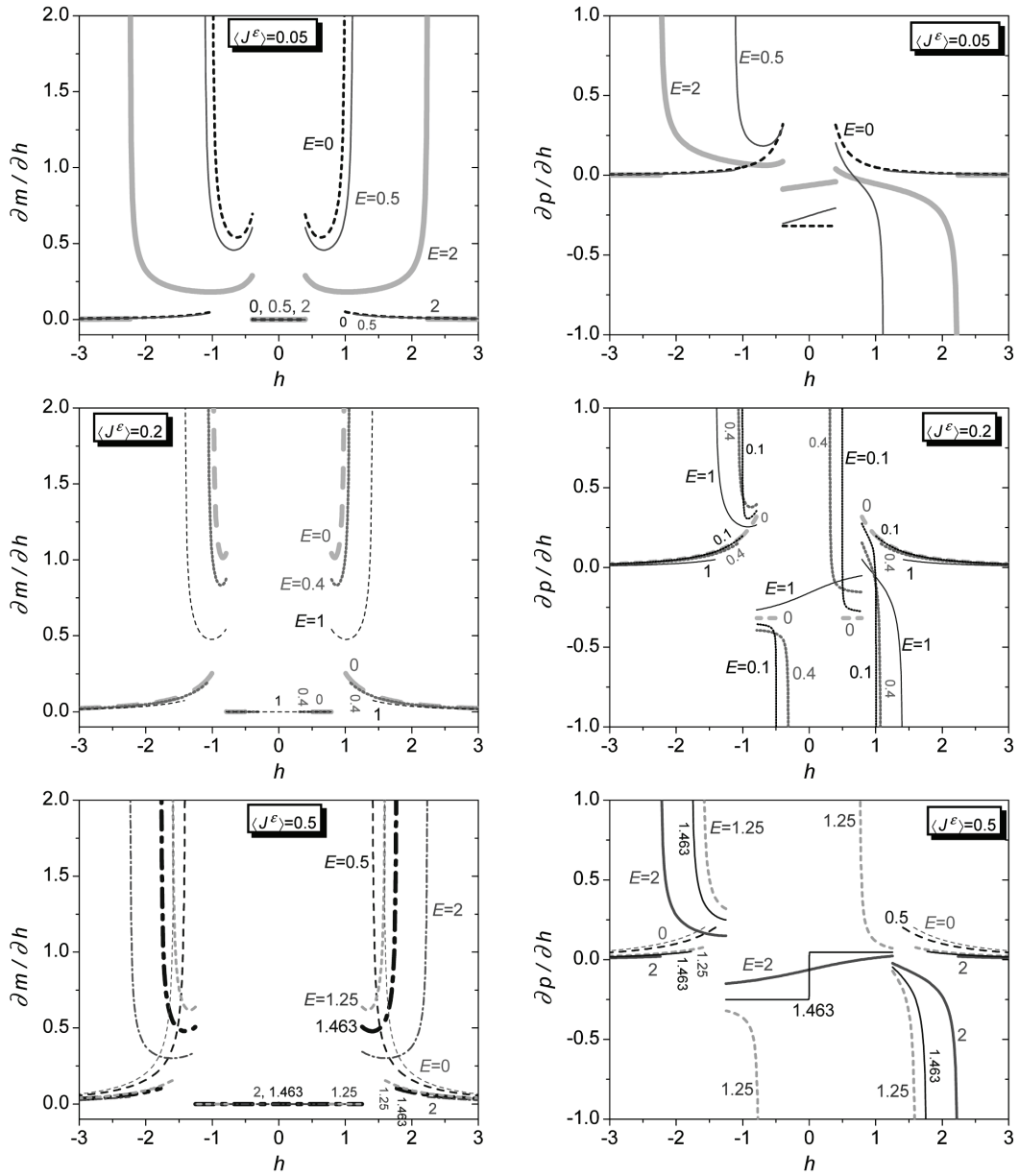

Fig. 7. Dependences of the magnetic, $\partial m/\partial h$, and magnetoelectric, $\partial p/\partial h$, susceptibilities on the magnetic field for various values of the energy flux and the electric field. The upper, middle, and lower figures correspond to $\langle J^{\mathcal{E}}\rangle = 0.05$, 0.2, and 0.5, respectively

and at the electric field values, when the system can only be in phase III (see Fig. 4, $\langle J^{\mathcal{E}}\rangle = 0.5$, $E = 0$ and 0.5). At large and growing $|h|$, the magnetization gradually saturates. Near the boundary of the region with no states, $m(h)$ increases drastically with h and goes to zero at the boundary of this region. Looking ahead, it should be noted that the behavior $m \to 0$ at the boundary of the region without states can also be seen in Fig. 5 (for $\langle J^{\mathcal{E}}\rangle = 0.5$ at $h = 1.3$ and 1.5) and in Fig. 6 (for $|E| = 0.5$ at $|h| = 1.5$ and 2, as well as for $|E| = 2$ at $|h| = 2.5$ and 3).

The behavior of the dependences $m(E)$ and $p(E)$ in various phases and at various phase transitions is illustrated in Fig. 5 (see also Figs. 2 and 3). In the

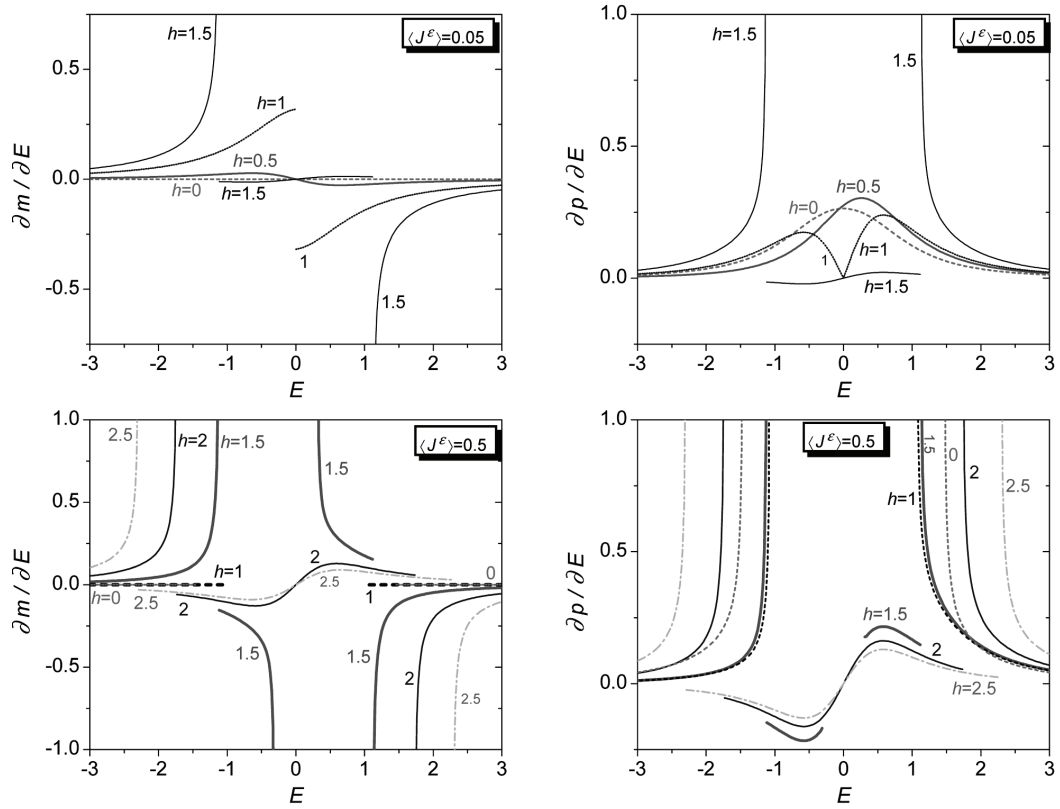

Fig. 8. Dependences of the magnetoelectric, $\partial m/\partial E$, and electric, $\partial p/\partial E$, susceptibilities on the electric field for various values of the energy flux and the magnetic field. The upper and lower figures correspond to $\langle J^{\mathcal{E}}\rangle = 0.05$ and 0.5, respectively

nonmagnetic phase I and the magnetically ordered phase II, the electric polarization increases with the electric field at both negative and positive E (with $p \to \pm 1/\pi$ at $E \to \pm\infty$ and provided that all other model parameters are finite). At the same time, in phase III, the dependence $p(E)$ is a decreasing function at $E < 0$ and an increasing one at $E > 0$, since the polarization in phase III is an even function of E. From the aforesaid, it is clear that, at the point of the II $\to$ III phase transition and the negative electric field values, $p(E)$ has a cusp and a maximum, whereas, at the point of the III $\to$ II phase transition and positive fields E, the polarization has a cusp, but not an extremum. It is of interest that, for the given magnetic field and the energy flux at the boundary of the region without states, the relation $p(E) = p(-E)$ is obeyed, not only when the system is in phase III (where the polarization is an even function of E), but also in phase I (see Fig. 5; for $\langle J^{\mathcal{E}}\rangle = 0.5$ at $h = 1.3$, 1.5, and 0.1).

Now, let us dwell very briefly on the dependence $m(E)$. Since it is an even function of the electric field, it is sufficient to confine its consideration to positive E-values. In this case, with the increasing electric field, the magnetization decreases in phase II and, on the contrary, increases in phase III.

All the aforesaid about the magnetization and polarization dependences on the electric field concerns only the cases of finite $h \geq 0$. The behavior of $m(E)$ and $p(E)$ at finite negative h can be seen from the properties $m(\mathcal{I}, h, E) = -m(\pm\mathcal{I}, -h, \pm E)$ and $p(\mathcal{I}, h, E) = -p(\mathcal{I}, -h, -E)$, which are obeyed provided that the energy flux is fixed.

Finally, let us consider the dependences of the magnetization, $m(\langle J^{\mathcal{E}}\rangle)$, and the electrical polarization, $p(\langle J^{\mathcal{E}}\rangle))$, at finite h and E (see Fig. 6, as well as Fig. 1 and 2). At rather large magnetic fields (e.g., at $|h| > 2.236$ for $|E| = 2$), the system is in the magnetically ordered phase III within the whole interval $\langle J^{\mathcal{E}}\rangle \in [0, \langle J^{\mathcal{E}}_{\max}\rangle]$ where the states exist. At

lower $|h|$-values and the increasing energy flux until $\langle J^{\mathcal{E}}\rangle < \langle J^{\mathcal{E}}_{\max}\rangle$, the phase transition from the magnetically ordered phase II to the magnetically disordered phase I takes place. In phases II and III, the dependence $p(\langle J^{\mathcal{E}}\rangle)$ is almost a linear function: decreasing at positive magnetic fields and increasing at negative ones. In those magnetically ordered phases, the following property for the polarization takes place, if the electric field is fixed: $p(\langle J^{\mathcal{E}}\rangle, h) = -p(\langle J^{\mathcal{E}}\rangle, -h) + 2p(0, |h|)$, with the value $p(0, h) = p(0, -h)$ being larger than zero (equal to zero) in phase II (III). In the nonmagnetic phase I, the polarization is a decreasing function of the energy flux for both positive and negative h.

All the aforesaid about the polarization dependences $p(\langle J^{\mathcal{E}}\rangle)$ is valid only for the cases with finite $E \geq 0$. The polarization behavior at finite negative E can be seen from the property $p(\langle J^{\mathcal{E}}\rangle, \mathcal{I}, h, E) = -p(\langle J^{\mathcal{E}}\rangle, \mathcal{I}, -h, -E)$.

The magnetization dependence $m(\langle J^{\mathcal{E}}\rangle)$ in the magnetically ordered phases is an expectedly decreasing (increasing) function at positive (negative) values of the magnetic field. It should be noted that the derivative $\partial m/\partial\langle J^{\mathcal{E}}\rangle$ in phase II in a vicinity of the transition II $\to$ I is a finite quantity, whereas it is infinitely large in phase III at $\langle J^{\mathcal{E}}\rangle \to \langle J^{\mathcal{E}}_{\max}\rangle$.

5.3. Susceptibilities

Now, let us briefly analyze the dependences of the magnetic, $\partial m/\partial h$, electric, $\partial p/\partial E$, and magnetoelectric, $\partial m/\partial E$ and $\partial p/\partial h$, susceptibilities on the magnetic and electric fields (see Figs. 7 and 8). The figures demonstrate all qualitatively different field dependences of the indicated susceptibilities.

Note that, from the symmetry properties of the magnetization and the electric polarization, one can easily see that $\partial m/\partial h$ is an even function of the superexchange interaction and the both fields. At the same time, $\partial m/\partial E$ is an odd function of h and E and an even function of $\mathcal{I}$. The susceptibility $\partial p/\partial h$ has the following property at a given energy flux: the simultaneous change of the directions of both fields does not vary this susceptibility, whereas the sign of $\partial p/\partial h$ changes to the opposite one, if the sign of the superexchange interaction and the direction of either of the fields change. The electrical susceptibility does not change, if the signs of any two parameters from the set ($\mathcal{I}$, h, and E) change.

Figures 7 and 8 demonstrate that all susceptibilities diverge in the magnetically ordered phase II at the boundary with another magnetically ordered phase III. The only exception is the case $|E| \to 0$ for $\partial p/\partial h$ (see Fig. 7, the curves for $\langle J^{\mathcal{E}}\rangle = 0.05$ and 0.2). It should be noted that the mechanism of the indicated differences in the susceptibility is known and similar to that taking place in the systems considered, e.g., in works [57, 90]. In addition, in a vicinity of the region without states, there are divergencies of the susceptibilities $\partial m/\partial h$ and $\partial m/\partial E$ in phase III, as well as $\partial p/\partial E$ and $\partial p/\partial h$ in the nonmagnetic phase I (except for the case $|E| \to 0$; see Fig. 7, the curves for $\langle J^{\mathcal{E}}\rangle = 0.2$).

In phase II, the magnetic susceptibility as a function of h is always nonmonotonic, whereas $\partial p/\partial h$ can be both a monotonic function and a nonmonotonic one of the magnetic field, depending on the model parameters (see Fig. 7). The electrical susceptibility, in turn, has a nonmonotonic dependence on the electric field with two extrema in phase III. The same can be said about $\partial m/\partial E$ in the same phase, but only for such h-values, when the given energy flux is achievable even at $E = 0$ (see Fig. 8, the curves for $\langle J^{\mathcal{E}}\rangle = 0.05$ at $h = 1.5$ and for $\langle J^{\mathcal{E}}\rangle = 0.5$ at $h = 2$ and 2.5).

It is important to pay attention to that the electrical susceptibilities in the magnetically ordered phase with two Fermi points can be negative (see Fig. 8). In our opinion, this occurs, because the unexpected effects are possible in the nonequilibrium steady states, e.g., negative heat capacity [93, 94].

6. Conclusions

In this work, the exact results are obtained for a number of parameters of the one-dimensional spin-$\frac{1}{2}$ XX model for a magnetoelectric with the steady energy flux. The latter is taken into account using the Lagrange multiplier method for quantum systems in the case of low temperatures. In this method, the nonequilibrium steady state is approximately considered as the ground state of the system, which is described by the effective Hamiltonian $\mathcal{H}^{\mathcal{E}} = \mathcal{H}^{\mathrm{ME}} - \lambda\mathcal{J}^{\mathcal{E}}$.

The phase diagrams were plotted in the magnetic field–energy flux, $(h, \langle J^{\mathcal{E}}\rangle)$, electric field–energy flux, $(E, \langle J^{\mathcal{E}}\rangle)$, and (E, h) planes. Differences in the behavior of the electric polarization p and the magneti-

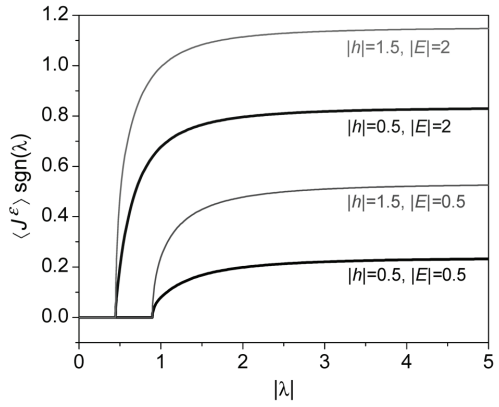

Fig. 9. Dependences of the energy flux $\langle J^{\mathcal{E}}\rangle$ on the governing field λ at $\mathcal{I} = |1|$ for various values of h and E

zation in different phases were found. Here is a short list of main conclusions that can be drawn from the study carried out for the finite positive $\langle J^{\mathcal{E}}\rangle$ and both positive and negative finite superexchange interaction values $\mathcal{I}$ and the fields h and E.

• The phase diagrams in the $h-\langle J^{\mathcal{E}}\rangle$ plane have the same topology at any electric field value. At the same time, both the $(E, \langle J^{\mathcal{E}}\rangle)$ and (E, h) diagrams can be qualitatively different at different h- and $\langle J^{\mathcal{E}}\rangle$-values, respectively. For instance, in the diagrams in the E – $\langle J^{\mathcal{E}}\rangle$ plane, the magnetically ordered phase with two Fermi points is present at large magnetic field magnitudes and is absent at its low values. In the (E, h) phase diagrams, the region without states is available only at sufficiently large energy flux values. In addition, the curves corresponding to the transitions between different phases do not intersect at small $\langle J^{\mathcal{E}}\rangle$, but at large flux values, they converge to the same point that lies on the boundary below which there are no states.

• In the phases with four Fermi points (the magnetically disordered I and magnetically disordered II ones), the polarization $p(E)$ is an increasing function. In the magnetically ordered phase III with two Fermi points, p increases with the electric field, if $hE\mathcal{I} < 0$ and decreases, if $hE\mathcal{I} > 0$. It is an even function of E only in this phase.

• The magnetization $m(E)$ in phase II decreases, if $hE > 0$, and increases, if $hE < 0$. On the contrary, in phase III, m is an increasing (decreasing) function of the field E at positive (negative) values of the field product.

• In nonmagnetic phase I, the polarization is a decreasing function of the energy flux, if $E > 0$, and an increasing one at negative E. In magnetically ordered phases II and III, $p(\langle J^{\mathcal{E}}\rangle)$ is an almost linear function: decreasing at $hI < 0$ and increasing at $hI > 0$.

• The dependence $m(\langle J^{\mathcal{E}}\rangle)$ in the magnetically ordered phase II is quite close to linear. The derivative $\partial m/\partial\langle J^{\mathcal{E}}\rangle$ in phase II in a vicinity of the II → I transition has a finite value.

• In the phases with four Fermi points (I and II), the polarization can be an increasing, decreasing, or nonmonotonic (with one extremum) function of the magnetic field at both positive and negative superexchange interaction values. At the same time, in the magnetically ordered phase III with two Fermi points, p can only increase with the growth of h at $\mathcal{I} < 0$ and decreases at $\mathcal{I} > 0$.

• If the energy flux $\langle J^{\mathcal{E}}\rangle$, rather than the flux-generating field λ, is considered as the problem parameter, the electric polarization $p(E)$ reaches the saturation $\pm 1/\pi$ at infinitely large E for any $\langle J^{\mathcal{E}}\rangle$-values. But if the field λ generating the energy flux is an independent variable (see work [65]), then $p(E) \to 0$ at $E \to \pm\infty$, except for the case $\lambda \to 0$, where $p(E) \to \pm 1/\pi$ at $E \to \pm\infty$.

• The magnetic, electric, and magnetoelectric susceptibilities diverge in phase II at the boundary with another magnetically ordered phase III. The only exception is the susceptibility $\partial p/\partial h$ at $|E| \to 0$.

• The magnetic susceptibility is always a nonmonotonic function of h in phase II, whereas $\partial p/\partial E$ must be a nonmonotonic function of the electric field in phase III.

The author expresses gratitude to T.M. Verkholyak for the interest in this work, help, advice, and useful discussion.

APPENDIX
Dependences of energy flux on the generating field

In the framework of the Lagrange multiplier method, the energy flux $\langle J^{\mathcal{E}}\rangle$ is an increasing and, naturally, an odd function of the governing field λ (see Fig. 9). Furthermore, $\langle J^{\mathcal{E}}_{\max}\rangle = \lim_{\lambda\to\infty}\langle J^{\mathcal{E}}(\lambda)\rangle$ is a finite quantity, which depends on the superexchange interaction, as well as the magnetic and electric fields. This means that, in the applied method, the system cannot achieve a flux larger than $\langle J^{\mathcal{E}}_{\max}(\mathcal{I}, h, E)\rangle$ under any circumstances.

The fact that the energy flux in the magnetoelectric model is finite for the given $\mathcal{I}$, h, and E can be verified analytically as well, proceeding from the expression for the local energy flux (6) in the operator form. The energy flux is the same ($\langle J_j^{\mathcal{E}}\rangle = \langle J^{\mathcal{E}}\rangle$) at every chain site. Then, on the basis of Eq. (6) after the fermionization, it is easy to obtain that

$$\langle J^{\mathcal{E}}\rangle = \frac{1}{2\pi}\int\limits_{-\pi}^{\pi} dk\Big[hE\cos k + h\mathcal{I}\sin k - E\mathcal{I}\cos(2k) + \\ + \frac{E^2 - \mathcal{I}^{\,2}}{2}\sin(2k)\Big]\langle n_k\rangle.$$

It is also worth to note that $\langle J^{\mathcal{E}}(\lambda, \mathcal{I}, h, E)\rangle$ is a single-valued function of the governing field (see Fig. 9). Therefore, it is not λ, but the conjugate parameter $\langle J^{\mathcal{E}}\rangle$ that is usually (for physical reasons) considered as an independent variable.

1. C.-Y. Hsieh, J. Liu, C. Duan, J. Cao. A Nonequilibrium variational polaron theory to study quantum heat transport. *J. Phys. Chem. C* **123**, 17196 (2019).
2. S. Saryal, H.M. Friedman, D. Segal, B.K. Agarwalla. Thermodynamic uncertainty relation in thermal transport. *Phys. Rev. E* **100**, 042101 (2019).
3. K.W. Becker, H. Fehske, V.N. Phan. Projector-based renormalization approach to electron-hole-photon systems in their nonequilibrium steady state. *Phys. Rev. B* **99**, 035304 (2019).
4. H. Ness. Nonequilibrium density matrix in quantum open systems: Generalization for simultaneous heat and charge steady-state transport. *Phys. Rev. E* **90**, 062119 (2014).
5. D.S. Kosov. Lagrange multiplier based transport theory for quantum wires. *J. Chem. Phys.* **120**, 7165 (2004).
6. G. Rastelli, W. Belzig. Ground state cooling of nanomechanical resonators by electron transport. *Eur. Phys. J. Spec. Top.* **227**, 1885 (2019).
7. D. Karevski, T. Platini. Quantum nonequilibrium steady states induced by repeated interactions. *Phys. Rev. Lett.* **102**, 207207 (2009).
8. T. Antal, Z. Rácz, L. Sasvári. Nonequilibrium steady state in a quantum system: One-dimensional transverse Ising model with energy current. *Phys. Rev. Lett.* **78**, 167 (1997).
9. T. Antal, Z. Rácz, A. Rákos, G.M. Schütz. Isotropic transverse XY chain with energy and magnetization currents. *Phys. Rev. E* **57**, 5184 (1998).
10. Z. Rácz. Presence of energy flow in quantum spin chains: An experimental signature. *J. Stat. Phys.* **101**, 273 (2000).
11. V. Eisler, Z. Rácz, F. van Wijland. Magnetization distribution in the transverse Ising chain with energy flow. *Phys. Rev. E* **67**, 056129 (2003).
12. V. Eisler, Z. Zimborás. Entanglement in the XX spin chain with an energy current. *Phys. Rev. A* **71**, 042318 (2005).
13. J. Hide. A steady state entanglement witness [https://arxiv.org/abs/1102.0220].
14. D. Karevski, R.J. Harris. Defect production in quench from a current-carrying nonequilibrium state. *J. Stat. Mech.: Theory Exp.* 033204 (2016).
15. C. Mejía-Monasterio, T. Prosen, G. Casati. Fourier's law in a quantum spin chain and the onset of quantum chaos. *Europhys. Lett.* **72**, 520 (2005).
16. W.H. Aschbacher, C.-A. Pillet. Nonequilibrium steady states of the XY chain. *J. Stat. Phys.* **112**, 1153 (2003).
17. Y. Ogata. Nonequilibrium properties in the transverse XX chain. *Phys. Rev. E* **66**, 016135 (2002).
18. D.L. González-Cabrera, Z. Rácz, F. van Wijland. Casimir effect in the nonequilibrium steady state of a quantum spin chain. *Phys. Rev. A* **81**, 052512 (2010).
19. M.O. Lavrentovich. Steady-state properties of coupled hot and cold Ising chains. *J. Phys. A* **45**, 085002 (2012).
20. X. Xu, K. Choo, V. Balachandran, D. Poletti. Transport and energetic properties of a ring of interacting spins coupled to heat baths. *Entropy* **21**, 228 (2019).
21. T. Antal, Z. Rácz, A. Rákos, G.M. Schütz. Transport in the XX chain at zero temperature: Emergence of flat magnetization profiles. *Phys. Rev. E* **59**, 4912 (1999).
22. M. Brenes, E. Mascarenhas, M. Rigol, J. Goold. High-temperature coherent transport in the XXZ chain in the presence of an impurity. *Phys. Rev. B* **98**, 235128 (2018).
23. J.L. Lancaster, J.P. Godoy. Persistence of power-law correlations in nonequilibrium steady states of gapped quantum spin chains. *Phys. Rev. Res.* **1**, 033104 (2019).
24. V. Popkov, T. Prosen, L. Zadnik. Exact nonequilibrium steady state of open XXZ/XYZ spin-1/2 chain with Dirichlet boundary conditions. *Phys. Rev. Lett.* **124**, 160403 (2020).
25. M. Rigol, V. Dunjko, V. Yurovsky, M. Olshanii. Relaxation in a completely integrable many-body quantum system: An ab initio study of the dynamics of the highly excited states of 1D lattice hard-core bosons. *Phys. Rev. Lett.* **98**, 050405 (2007).
26. E. Ilievski, J. De Nardis, B. Wouters, J.-S. Caux, F.H.L. Essler, T. Prosen. Complete generalized gibbs ensembles in an interacting theory. *Phys. Rev. Lett.* **115**, 157201 (2015).
27. D. Liu, Y. Zhang, Y. Liu, G.-L. Long. Entanglement in the ground state of an isotropic three-qubit transverse XY chain with energy current. *Chin. Phys. Lett.* **24**, 8 (2007).
28. B.-Q. Liu, B. Shao, J. Zou. Entanglement of two qubits coupled to an XY spin chain: Role of energy current. *Phys. Rev. A* **80**, 062322 (2009).
29. Z.-M. Wang, B. Shao, P. Chang, J. Zou. Quantum state transfer in a Heisenberg XY chain with energy current. *Physica A* **387**, 2197 (2008).
30. Y.-C. Qiu, Q.-Q. Wu, W.-L. You. Energy dynamics in a generalized compass chain. *J. Phys.: Condens. Matter* **28**, 496001 (2016).
31. M. Fiebig. Revival of the magnetoelectric effect. *J. Phys. D* **38**, R123 (2005).
32. M. Fiebig, T. Lottermoser, D. Meier, M. Trassin. The evolution of multiferroics. *Nat. Rev. Mater.* **1**, 16046 (2016).
33. K.F. Wang, J.-M. Liu, Z.F. Ren. Multiferroicity: the coupling between magnetic and polarization orders. *Adv. Phys.* **58**, 321 (2009).

34. Y. Tokura, Sh. Seki, N. Nagaosa. Multiferroics of spin origin. *Rep. Prog. Phys.* **77**, 076501 (2014).
35. D.I. Khomskii. *Transition Metal Compounds* (Cambridge University Press, 2014).
36. I.V. Solovyev, T.V. Kolodiazhnyi. Experimental and first-principles studies of magnetism and magnetoelectric effect in $Co_4Nb_2O_9$ and $Co_4Ta_2O_9$. *Phys. Rev. B* **94**, 094427 (2016).
37. *Multiferroic Materials: Properties, Techniques, and Applications.* Edited by J. Wang (CRC Press, 2017).
38. E.A. Eliseev, A.N. Morozovska, M.D. Glinchuk, B.Y. Zaulychny, V.V. Skorokhod, R. Blinc. Surface-induced piezomagnetic, piezoelectric, and linear magnetoelectric effects in nanosystems. *Phys. Rev. B* **82**, 085408 (2010).
39. M.D. Glinchuk, E.A. Eliseev, Y. Gu, L.-Q. Chen, V. Gopalan, A.N. Morozovska. Electric-field induced ferromagnetic phase in paraelectric antiferromagnets. *Phys. Rev. B* **89**, 014112 (2014).
40. M.D. Glinchuk, V.V. Khist. Renovation of interest in the magnetoelectric effect in nanoferroics. *Ukr. J. Phys.* **13**, 1006 (2018).
41. I.E. Dzyaloshinskii. On the magneto-electrical effect in antiferromagnets. *Sov. Phys. JETP* **10**, 628 (1960).
42. D.N. Astrov. The magnetoelectric effect in antiferromagnetics. *Sov. Phys. JETP* **11**, 708 (1960).
43. H. Katsura, N. Nagaosa, A.V. Balatsky. Spin current and magnetoelectric effect in noncollinear magnets. *Phys. Rev. Lett.* **95**, 057205 (2005).
44. I.A. Sergienko, E. Dagotto. Role of the Dzyaloshinskii–Moriya interaction in multiferroic perovskites. *Phys. Rev. B* **73**, 094434 (2006).
45. S. Seki, T. Kurumaji, S. Ishiwata, H. Matsui, H. Murakawa, Y. Tokunaga, Y. Kaneko, T. Hasegawa, Y. Tokura. Cupric chloride $CuCl_2$ as an $S = 1/2$ chain multiferroic. *Phys. Rev. B* **82**, 064424 (2010).
46. S. Seki, Y. Yamasaki, M. Soda, M. Matsuura, K. Hirota, Y. Tokura. Correlation between spin helicity and an electric polarization vector in quantum-spin chain magnet $LiCu_2O_2$. *Phys. Rev. Lett.* **100**, 127201 (2008).
47. F. Schrettle, S. Krohns, P. Lunkenheimer, J. Hemberger, N. Büttgen, H.-A. Krug von Nidda, A.V. Prokofiev, A. Loidl. Switching the ferroelectric polarization in the $S = 1/2$ chain cuprate $LiCuVO_4$ by external magnetic fields. *Phys. Rev. B* **77**, 144101 (2008).
48. Y. Wang, J. Li, D. Viehland. Magnetoelectrics for magnetic sensor applications: status, challenges and perspectives. *Materials Today* **17**, 269 (2014).
49. N. Ortega, A. Kumar, J.F. Scott, R.S. Katiyar. Multifunctional magnetoelectric materials for device applications. *J. Phys.: Condens. Matter* **27**, 504002 (2015).
50. F. Matsukura, Y. Tokura, H. Ohno. Control of magnetism by electric fields. *Nature Nanotechnol.* **10**, 209 (2015).
51. I. Kézsmárki, U. Nagel, S. Bordács, R.S. Fishman, J.H. Lee, H.T. Yi, S-W. Cheong, T. Rõõm. Optical diode effect in the room-temperature multiferroic $BiFeO_3$. *Phys. Rev. Lett.* **115**, 127203 (2015).
52. M. Sato, Sh. Takayoshi, T. Oka. Laser-driven multiferroics and ultrafast spin current generation. *Phys. Rev. Lett.* **117**, 147202 (2016).
53. D.M. Juraschek, M. Fechner, A.V. Balatsky, N.A. Spaldin. Dynamical multiferroicity. *Phys. Rev. Materials* **1**, 014401 (2017).
54. M. Azimi, M. Sekania, S.K. Mishra, L. Chotorlishvili, Z. Toklikishvili, J. Berakdar. Pulse and quench induced dynamical phase transition in a chiral multiferroic spin chain. *Phys. Rev. B* **94**, 064423 (2016).
55. M. Brockmann, A. Klümper, V. Ohanyan. Exact description of magnetoelectric effect in the spin-1/2 XXZ chain with Dzyaloshinskii–Moriya interaction. *Phys. Rev. B* **87**, 054407 (2013).
56. O. Menchyshyn, V. Ohanyan, T. Verkholyak, T. Krokhmalskii, O. Derzhko. Magnetism-driven ferroelectricity in spin-$\frac{1}{2}$ XY chains. *Phys. Rev. B* **92**, 184427 (2015).
57. O. Baran, V. Ohanyan, T. Verkholyak. Spin-1/2 XY chain magnetoelectric: Effect of zigzag geometry. *Phys. Rev. B* **98**, 064415 (2018).
58. V. Ohanyan. Influence of XY anisotropy on a magnetoelectric effect in spin-1/2 XY chain in a transverse magnetic field. *Condens. Matter Phys.* **23**, 43704 (2020).
59. J. Strečka, L. Gálisová, T. Verkholyak. Enhanced magnetoelectric effect near a field-driven zero-temperature quantum phase transition of the spin-1/2 Heisenberg-Ising ladder. *Phys. Rev. E* **101**, 012103 (2020).
60. W.-L. You, G.-H. Liu, P. Horsch, A.M. Oleś. Exact treatment of magnetism-driven ferroelectricity in the one-dimensional compass model. *Phys. Rev. B* **90**, 094413 (2014).
61. H. Čenčariková, J. Strečka. Enhanced magnetoelectric effect of the exactly solved spin-electron model on a doubly decorated square lattice in the vicinity of a continuous phase transition. *Phys. Rev. E* **98**, 062129 (2018).
62. K. Saito, S. Takesue, S. Miyashita. Thermal conduction in a quantum system. *Phys. Rev. E* **54**, 2404 (1996).
63. X. Zotos, F. Naef, P. Prelovšek. Transport and conservation laws. *Phys. Rev. B* **55**, 11029 (1997).
64. A. Klümper, K. Sakai. The thermal conductivity of the spin-$\frac{1}{2}$ XXZ chain at arbitrary temperature. *J. Phys. A: Math. Gen.* **35**, 2173 (2002).
65. O.R. Baran. *Energy current effect in the one-dimensional spin-1/2 XX model of the magnetoelectric. Lagrange multiplier method.* Preprint ICMP-20-06U (Lviv, 2020) [http://www.icmp.lviv.ua/preprints/2020/20-06u].
66. I.E. Dzialoshinskii. Thermodynamic theory of "weak" ferromagnetism in antiferromagnetic substances. *Sov. Phys. JETP* **5**, 1259 (1957).
67. T. Moriya. Anisotropic superexchange interaction and weak ferromagnetism. *Phys. Rev.* **120**, 91 (1960).
68. V.M. Kontorovich, V.M. Tsukernik. Spiral structure in a one-dimensional chain of spins. *Sov. Phys. JETP* **25**, 960 (1967).
69. V.N. Krivoruchko. Magnon bound-states in an anisotropic chain of spin with the Dzyaloshinskii interaction. *Fiz. Nizk. Temp.* **12**, 872 (1986).

70. A.A. Zvyagin. The ground-state structure of a spin chain with the Dzyaloshinsky type interaction. *Fiz. Nizk. Temp.* **15**, 977 (1989).
71. O.V. Derzhko, A.Ph. Moina. Statistical mechanics of one-dimensional $s = 1/2$ anisotropic XY model in transverse field with Dzyaloshinskii–Moriya interaction. *Condens. Matter Phys.* No 3, 3 (1994).
72. O. Derzhko, A. Moina. $1D$ $S = 1/2$ anisotropic XY model in transverse field with Dzyaloshinskii–Moriya interaction. *Ferroelectrics* **153**, 49 (1994).
73. O. Derzhko, T. Verkholyak. Effects of Dzyaloshinskii-Moriya interaction in the dynamics of $s = 1/2$ XX chain. *Czech. J. Phys.* **54**, D531 (2004).
74. O. Derzhko, T. Verkholyak, T. Krokhmalskii, H. Büttner. Dynamic probes of quantum spin chains with the Dzyaloshinskii–Moriya interaction. *Phys. Rev. B* **73**, 214407 (2006).
75. O. Derzhko, T. Verkholyak. Dynamic structure factors of the spin-1/2 XX chain with Dzyaloshinskii–Moriya interaction. *J. Phys. Soc. Jpn.* **75**, 104711 (2006).
76. N. Avalishvili, B. Beradze, G.I. Japaridze. Magnetic phase diagram of a spin S=1/2 antiferromagnetic two-leg ladder with modulated along legs Dzyaloshinskii–Moriya interaction. *Eur. Phys. J. B* **92**, 262 (2019).
77. F.K. Fumani, B. Beradze, S. Nemati, S. Mahdavifar, G.I. Japaridze. Quantum correlations in the spin-1/2 Heisenberg XXZ chain with modulated Dzyaloshinskii–Moriya interaction. *J. Magn. Magn. Mater.* **518**, 167411 (2021).
78. F. Heidrich-Meisner, A. Honecker, D.C. Cabra, W. Brenig. Zero-frequency transport properties of one-dimensional spin-$\frac{1}{2}$ systems. *Phys. Rev. B* **68**, 134436 (2003).
79. M. Michel, O. Hess, H. Wichterich, J. Gemmer. Transport in open spin chains: A Monte Carlo wave-function approach. *Phys. Rev. B* **77**, 104303 (2008).
80. L.-A. Wu, D. Segal. Energy flux operator, current conservation and the formal Fourier's law. *J. Phys. A.* **42**, 025302 (2009).
81. R. Steinigeweg, J. Gemmer, W. Brenig. Spin and energy currents in integrable and nonintegrable spin-$\frac{1}{2}$ chains: A typicality approach to real-time autocorrelations. *Phys. Rev. B* **91**, 104404 (2015).
82. A.M. Tsvelik. Incommensurate phases of quantum one-dimensional magnetics. *Phys. Rev. B* **42**, 779 (1990).
83. A.A. Zvyagin, A. Klümper. Quantum phase transitions and thermodynamics of quantum antiferromagnets with next-nearest-neighbor couplings. *Phys. Rev. B* **68**, 144426 (2003).
84. H. Frahm. Integrable spin-1/2 XXZ Heisenberg chain with competing interactions. *J. Phys. A* **25**, 1417 (1992).
85. I. Titvinidze, G.I. Japaridze. Phase diagram of the spin $S = 1/2$ extended XY model. *Eur. Phys. J. B* **32**, 383 (2003).
86. T. Krokhmalskii, O. Derzhko, J. Stolze, T. Verkholyak. Dynamic properties of the spin-$\frac{1}{2}$ XY chain with three-site interactions. *Phys. Rev. B* **77**, 174404 (2008).
87. M. Topilko, T. Krokhmalskii, O. Derzhko, V. Ohanyan. Magnetocaloric effect in spin-1/2 XX chains with three-spin interactions. *Eur. Phys. J. B* **85**, 278 (2012).
88. E. Lieb, T. Schultz, D. Mattis. Two soluble models of an antiferromagnetic chain. *Ann. Phys. (N.Y.)* **16**, 407 (1961).
89. O. Derzhko. Jordan–Wigner fermionization for spin–$\frac{1}{2}$ systems in two dimensions: A brief review. *J. Phys. Studies* **5** No. 1, 49 (2001).
90. T. Krokhmalskii, T. Verkholyak, O. Baran, V. Ohanyan, O. Derzhko. Spin-$\frac{1}{2}$ XX chain in a transverse field with regularly alternating g factors: Static and dynamic properties. *Phys. Rev. B* **102**, 144403 (2020).
91. M. Fabrizio. Superconductivity from doping a spin-liquid insulator: A simple one-dimensional example. *Phys. Rev. B* **54**, 10054 (1996).
92. A.A. Zvyagin. Quantum phase transitions in low-dimensional quantum spin systems with incommensurate magnetic structures. *Phys. Rev. B* **72**, 064419 (2005).
93. R.K.P. Zia, E.L. Praestgaard, O.G. Mouritsen. Getting more from pushing less: Negative specific heat and conductivity in nonequilibrium steady states. *Am. J. Phys.* **70**, 384 (2002).
94. E. Boksenbojm, C. Maes, K. Netočný, J. Pešek. Heat capacity in nonequilibrium steady states. *Europhys. Lett.* **96**, 40001 (2011).

Received 26.02.21.
Translated from Ukrainian by O.I. Voitenko

О.Р. Баран

ЕФЕКТ ПОТОКУ ЕНЕРГІЇ В ОДНОВИМІРНІЙ СПІН-1/2 XX МОДЕЛІ МАГНЕТОЕЛЕКТРИКА. МЕТОД МНОЖНИКА ЛАГРАНЖА

Для дослідження нерівноважних стаціонарних станів з потоком енергії одновимірної спін-1/2 XX моделі магнетоелектрика з механізмом Кацури–Наґаоси–Балацького при достатньо низьких температурах використано метод множника Лагранжа. За допомогою перетворення Йордана–Віґнера задача зводиться до гамільтоніана невзаємодіючих безспінових ферміонів і може бути розв'язаною точно. Побудовано ряд фазових діаграм та розраховано залежності намагніченості, електричної поляризації та різноманітних сприйнятливостей від магнітного та електричного полів, а також і від потоку енергії.

Ключові слова: одновимірна XX модель, магнетоелектрик, нерівноважні стаціонарні стани, потік енергії, метод множника Лагранжа.